Supporting Materials for

Composition and Reactivity of Volatile Organic Compounds in the South Coast Air Basin and San Joaquin Valley of California

1 Methods

This section presents the details of the measurements used in this study.

1.1 O_3 and NO_x measured by chemiluminescence

O_3 and NO_x were measured by chemiluminescence (CL) (Bourgeois et al., 2022; Bourgeois et al., 2021). Ambient O_3 was reacted with pure NO, and the resulting CL signal was detected, amplified, and converted to ambient levels based on ground and in-flight calibrations by standard additions of O_3 generated on board the aircraft. Ambient NO was reacted with onboard-generated O_3 and the resulting CL signal was converted to ambient levels in a similar method as for O_3, but calibrated with standard additions from an NO standard. NO_2 was converted to NO by UV photolysis at 385 nm, and detected similarly to NO. O_3 , NO, and NO_2 were reported at 1-Hz with an uncertainty and precision of ±(2% + 15 pptv), ±(4% + 6 pptv), and ±(7% + 20 pptv) for O_3, NO, and NO_2, respectively.

1.2 CO and CH_4 measured by laser absorption spectroscopy

CO and CH_4 were measured using the Differential Absorption Carbon monOxide Measurement DACOM instrument (Sachse et al., 1987). This instrument utilizes three single-mode tunable diode lasers, with CO measured using a quantum cascade laser (QCL) at approximately 4.7 μm and CH_4 with an interband cascade laser (ICL) at ~3.3 μm.

The DACOM instrument was calibrated, using gases supplied by NOAA ESRL, nominally on a 4-minute clock, but often advanced or delayed in time to avoid calibrating during fire plume encounters. Calibrations provided both slope and intercept values tying signals to species concentrations. Post-campaign analysis of the DACOM CO data indicated that measurement precision (1σ) was approximately 0.1% at 1 Hz and 0.14% at 5 Hz. CO

accuracy was dependent on the degree of nonlinearity in the signal, and varied from 2% to 7%. Short-term CH_4 precision was approximately 0.1% at 1 Hz and 0.2% at 5 Hz, and CH_4 accuracy was 1%.

1.3 Non-methane VOCs measured from the University of California Irvine whole air samples (UC Irvine WAS)

Most VOCs were measured offline by the Blake laboratory at UC Irvine. These measurements serve as the backbone with which other measurements are merged. The whole air samples (WAS) were collected between ~11:00 and 18:00 (local time) using 2-L canisters when the planetary boundary layer was around its maximum height (Zhong et al., 2004). The sampling duration ranged from 20 s to 100 s, with an average of 40 s. The samples were sent to UCI for analysis after collection. A multi-column/detector gas chromatography (GC) system was used to quantify the VOCs (Simpson et al., 2020). A detailed description of the analytical technique can be found in the work of Simpson et al. (2020). Briefly, the sample is first cryogenically pre-concentrated to allow the detection of species in the part-per-trillion by volume (pptv) range. The sample is subsequently vaporized and split into five different streams directed to a multi-column/detector GC system. The system consists of three Hewlett-Packard 6890 GC units. The first GC is equipped with two different columns that output to an electron capture detector (ECD) and a Flame Ionization Detector (FID). The second GC outputs to an FID. The third GC is equipped with two different columns that output to a quadrupole mass spectrometer (Q-MS) detector working in selected ion monitoring (SIM) mode and an ECD.

A total of five different column/detector combinations allowed for the identification and the quantification of different classes of compounds, including selected sulfur compounds, C_2-C_5 alkyl nitrates, C_2-C_{10} hydrocarbons, C_2-C_{10} oxygenated VOCs (OVOCs), and a wide variety of halogenated compounds.

The measurement precision, detection limits, and accuracy vary by the compound. The detection limit is 3 pptv for non-methane hydrocarbons (NMHCs). The accuracy, precision, and limit of detection (LOD) for each individual species measured in the canister samples

can be found in the NASA FIREX-AQ data archive (https://www-air.larc.nasa.gov/cgi-bin/ArcView/firexaq).

1.4 Non-methane VOCs measured by the HR-ToF-GC/MS

Non-methane VOCs were measured using the National Center for Atmospheric Research (NCAR) Trace Organic Gas Analyzer (TOGA) with Time-of-Flight mass spectrometer (TOGA-TOF). The TOGA-TOF is a fast-online gas chromatography-mass spectrometry (GC-MS) that is used to make airbone measurements of a large number of VOC mixing ratios. During these FIREX-AQ flights, TOGA was typically used to sample ambient air for 33 s every 105 s continuously during flight. The TOGA-TOF was routinely calibrated in flight during FIREX-AQ and before and after the deployments in the laboratory using a catalytic-clean air generator/dynamic dilution system with accurate (±1%) and precise (±1%) calibration gas delivery. The system operates continuously, allowing for frequent calibrations and zeros during flight. TOGA-TOF VOC detection limits are species dependent, generally 0.3–1 ppt for NMHC and halogenated VOCs, and 0.5-5 ppt for OVOCs. Measurement uncertainties are also species dependent, but typically 20%, with measurement precision 3% or less. The TOGA system is described in detail in Apel et al. (2015).

1.5 Non-methane VOCs measured from the NOAA Integrated Whole Air Sampling system (NOAA iWAS)

The NOAA (National Oceanic and Atmospheric Administration) iWAS flight system is capable of collecting a maximum of 72 whole air samples per flight with offline analysis by a custom-built, two-channel, GC-MS instrument described in detail in Lerner et al. (2017). The NOAA iWAS system features fast-fill, on-demand sampling using a computer interface. Each 1.4 L electropolished stainless steel canister is filled during flight from a starting pressure of 0.01 torr (1.3 Pa) to 2300 torr (3.1×10^5 Pa) in approximately 5 seconds during the California-based research flights during FIREX-AQ. There were 35 iWAS samples collected at low altitude in the SJV with the aim of surveying the entire basin by collecting multiple samples centered on each east/west leg of the raster pattern. There were 90 samples collected at low altitude, over land in the SoCab where the majority of the

samples were collected on the east/west segment parallel to Interstate 10. The flight operator would used real-time information from the NOAA PTR-MS and carbon monoxide measurements to primarily target VOC plumes in each region.

1.6 HCHO measured by the laser absorption spectroscopy

Continuous (1s) measurement of HCHO was acquired by the University of Colorado's Compact Atmospheric Multi-species Spectrometer (CAMS). Comprehensive details of this instrument can be found in Richter et al. (2015) and Fried et al. (2020), and only a brief overview is provided here. Ambient air is continuously sampled through a heated HIMML inlet, through PFA Teflon tubing, and through a multi-pass absorption cell employing flow rates around 5.2 standard liters per minute (slpm). Mid-infrared light at 3.53-μm (2831.6 cm^{-1}) was generated to access the moderately strong and largely isolated absorption feature of HCHO. The laser wavelenth was directed through the multi-pass cell, and after achieving a pathlength of 89.7-m, the absorbed laser power was measured. Zero-air, generated employing a pair of on-board scrubbers, was periodically acquired approximately every 10-min to remove optical background features and residual inlet/cell outgassing. The absorption signals were calibrated employing standards sampled prior to every flight and measured using direct absorption spectroscopy with the Beers-Lambert Absorption Law. During FIREX-AQ, the 1-s, 1-σ limit of detection for HCHO produced median values of 115 pptv and estimated accuracy of 6%.

1.7 Non-methane VOCs measured by the chemical ionization mass spectrometery (CIMS)

The CIMS technique allows simultaneous measurement of a variety of non-methane VOCs with high time resolution. In the CIMS instrument, the gaseous analytes are ionized by the reagent ions via ion-molecular reactions, followed by detection and quantification with a mass spectrometer. Various reagent ions can be used to selectively measure chemicals with different functionalities. The CIMS measurements provided by NOAA, Georgia Tech, and CalTech were used in this study. Detailed descriptions of the instruments can be found from previous studies (Yuan et al., 2017; Crounse et al., 2006; Veres et al., 2020; Zheng et al., 2011).

References

Apel, E., Hornbrook, R., Hills, A., Blake, N., Barth, M., Weinheimer, A., Cantrell, C., Rutledge, S., Basarab, B., and Crawford, J.: Upper tropospheric ozone production from lightning NOx - impacted convection: Smoke ingestion case study from the DC3 campaign, Journal of Geophysical Research: Atmospheres, 120, 2505-2523, 2015.

Bourgeois, I., Peischl, J., Neuman, J. A., Brown, S. S., Allen, H. M., Campuzano-Jost, P., Coggon, M. M., DiGangi, J. P., Diskin, G. S., and Gilman, J. B.: Comparison of airborne measurements of NO, NO2, HONO, NOy and CO during FIREX-AQ, Atmospheric Measurement Techniques Discussions, 1-47, 2022.

Bourgeois, I., Peischl, J., Neuman, J. A., Brown, S. S., Thompson, C. R., Aikin, K. C., Allen, H. M., Angot, H., Apel, E. C., and Baublitz, C. B.: Large contribution of biomass burning emissions to ozone throughout the global remote troposphere, Proceedings of the National Academy of Sciences, 118, 2021.

Crounse, J. D., McKinney, K. A., Kwan, A. J., and Wennberg, P. O.: Measurement of gas-phase hydroperoxides by chemical ionization mass spectrometry, Analytical chemistry, 78, 6726-6732, 2006.

Dolgorouky, C., Gros, V., Sarda-Esteve, R., Sinha, V., Williams, J., Marchand, N., Sauvage, S., Poulain, L., Sciare, J., and Bonsang, B.: Total OH reactivity measurements in Paris during the 2010 MEGAPOLI winter campaign, Atmospheric Chemistry and Physics, 12, 9593-9612, 10.5194/acp-12-9593-2012, 2012.

Fried, A., Walega, J., Weibring, P., Richter, D., Simpson, I. J., Blake, D. R., Blake, N. J., Meinardi, S., Barletta, B., and Hughes, S. C.: Airborne formaldehyde and volatile organic compound measurements over the Daesan petrochemical complex on Korea's northwest coast during the Korea-United States Air Quality study: Estimation of emission fluxes and effects on air quality, Elementa: Science of the Anthropocene, 8, 2020.

Gilman, J. B., Kuster, W. C., Goldan, P. D., Herndon, S. C., Zahniser, M. S., Tucker, S. C., Brewer, W. A., Lerner, B. M., Williams, E. J., Harley, R. A., Fehsenfeld, F. C., Warneke, C., and de Gouw, J. A.: Measurements of volatile organic compounds during the 2006 TexAQS/GoMACCS campaign: Industrial influences, regional characteristics, and diurnal dependencies of the OH reactivity, Journal of Geophysical Research, 114, 10.1029/2008jd011525, 2009.

Heald, C. L. and Kroll, J. H.: The fuel of atmospheric chemistry: Toward a complete description of reactive organic carbon, Sci Adv, 6, eaay8967, 10.1126/sciadv.aay8967, 2020.

Heald, C. L., Gouw, J., Goldstein, A. H., Guenther, A. B., Hayes, P. L., Hu, W., Isaacman-VanWertz, G., Jimenez, J. L., Keutsch, F. N., Koss, A. R., Misztal, P. K., Rappengluck, B., Roberts, J. M., Stevens, P. S., Washenfelder, R. A., Warneke, C., and Young, C. J.: Contrasting reactive organic carbon observations in the southeast United States (SOAS) and southern California (CalNex), Environ Sci Technol, 54, 14923-14935, 10.1021/acs.est.0c05027, 2020.

Kim, S., Jeong, D., Sanchez, D., Wang, M., Seco, R., Blake, D., Meinardi, S., Barletta, B., Hughes, S., Jung, J., Kim, D., Lee, G., Lee, M., Ahn, J., Lee, S.-D., Cho, G., Sung, M.-Y., Lee,

Y.-H., and Park, R.: The controlling factors of photochemical ozone production in Seoul, South Korea, Aerosol and Air Quality Research, 18, 2253-2261, 10.4209/aaqr.2017.11.0452, 2018.

Lee, J. D., Young, J. C., Read, K. A., Hamilton, J. F., Hopkins, J. R., Lewis, A. C., Bandy, B. J., Davey, J., Edwards, P., Ingham, T., Self, D. E., Smith, S. C., Pilling, M. J., and Heard, D. E.: Measurement and calculation of OH reactivity at a United Kingdom coastal site, Journal of Atmospheric Chemistry, 64, 53-76, 10.1007/s10874-010-9171-0, 2010.

Lerner, B. M., Gilman, J. B., Aikin, K. C., Atlas, E. L., Goldan, P. D., Graus, M., Hendershot, R., Isaacman-VanWertz, G. A., Koss, A., and Kuster, W. C.: An improved, automated whole air sampler and gas chromatography mass spectrometry analysis system for volatile organic compounds in the atmosphere, Atmospheric Measurement Techniques, 10, 291-313, 2017.

Ling, Z. H., Guo, H., Lam, S. H. M., Saunders, S. M., and Wang, T.: Atmospheric photochemical reactivity and ozone production at two sites in Hong Kong: Application of a Master Chemical Mechanism-photochemical box model, Journal of Geophysical Research: Atmospheres, 119, 10567-10582, 10.1002/2014jd021794, 2014.

Mao, J., Ren, X., Brune, W., Olson, J., Crawford, J., Fried, A., Huey, L., Cohen, R., Heikes, B., and Singh, H.: Airborne measurement of OH reactivity during INTEX-B, Atmospheric Chemistry and Physics, 9, 163-173, 2009.

Mao, J., Ren, X., Chen, S., Brune, W. H., Chen, Z., Martinez, M., Harder, H., Lefer, B., Rappenglück, B., Flynn, J., and Leuchner, M.: Atmospheric oxidation capacity in the summer of Houston 2006: Comparison with summer measurements in other metropolitan studies, Atmospheric Environment, 44, 4107-4115, 10.1016/j.atmosenv.2009.01.013, 2010.

Richter, D., Weibring, P., Walega, J. G., Fried, A., Spuler, S. M., and Taubman, M. S.: Compact highly sensitive multi-species airborne mid-IR spectrometer, Applied Physics B, 119, 119-131, 2015.

Sachse, G. W., Hill, G. F., Wade, L. O., and Perry, M. G.: Fast‐response, high‐precision carbon monoxide sensor using a tunable diode laser absorption technique, Journal of Geophysical Research: Atmospheres, 92, 2071-2081, 1987.

Sadanaga, Y., Yoshino, A., Kato, S., and Kajii, Y.: Measurements of OH reactivity and photochemical ozone production in the urban atmosphere, Environmental science & technology, 39, 8847-8852, 2005.

Simpson, I. J., Blake, D. R., Blake, N. J., Meinardi, S., Barletta, B., Hughes, S. C., Fleming, L. T., Crawford, J. H., Diskin, G. S., and Emmons, L. K.: Characterization, sources and reactivity of volatile organic compounds (VOCs) in Seoul and surrounding regions during KORUS-AQ, Elementa: Science of the Anthropocene, 8, 2020.

Steiner, A., Cohen, R., Harley, R., Tonse, S., Millet, D., Schade, G., and Goldstein, A.: VOC reactivity in central California: comparing an air quality model to ground-based measurements, Atmospheric Chemistry and Physics, 8, 351-368, 2008.

Thames, A. B., Brune, W. H., Miller, D. O., Allen, H. M., Apel, E. C., Blake, D. R., Bui, T. P., Commane, R., Crounse, J. D., Daube, B. C., Diskin, G. S., DiGangi, J. P., Elkins, J. W., Hall, S. R., Hanisco, T. F., Hannun, R. A., Hintsa, E., Hornbrook, R. S., Kim, M. J., McKain, K., Moore,

F. L., Nicely, J. M., Peischl, J., Ryerson, T. B., St. Clair, J. M., Sweeney, C., Teng, A., Thompson, C. R., Ullmann, K., Wennberg, P. O., and Wolfe, G. M.: Missing OH reactivity in the global marine boundary layer, Atmospheric Chemistry and Physics, 20, 4013-4029, 10.5194/acp-20-4013-2020, 2020.

Veres, P. R., Neuman, J. A., Bertram, T. H., Assaf, E., Wolfe, G. M., Williamson, C. J., Weinzierl, B., Tilmes, S., Thompson, C. R., and Thames, A. B.: Global airborne sampling reveals a previously unobserved dimethyl sulfide oxidation mechanism in the marine atmosphere, Proceedings of the National Academy of Sciences, 117, 4505-4510, 2020.

Wu, R. and Xie, S.: Spatial distribution of ozone formation in China derived from emissions of speciated volatile organic compounds, Environmental science & technology, 51, 2574-2583, 2017.

Yuan, B., Koss, A. R., Warneke, C., Coggon, M., Sekimoto, K., and de Gouw, J. A.: Proton-transfer-reaction mass spectrometry: Applications in atmospheric sciences, Chemical Reviews, 117, 13187-13229, 2017.

Zheng, W., Flocke, F., Tyndall, G., Swanson, A., Orlando, J., Roberts, J., Huey, L., and Tanner, D.: Characterization of a thermal decomposition chemical ionization mass spectrometer for the measurement of peroxy acyl nitrates (PANs) in the atmosphere, Atmospheric Chemistry and Physics, 11, 6529-6547, 2011.

Zhong, S., Whiteman, C. D., and Bian, X.: Diurnal evolution of three-dimensional wind and temperature structure in California's Central Valley, Journal of Applied Meteorology, 43, 1679-1699, 2004.

Table S1. Comparison of the calculated OHR (s^{-1}) in this study with other regions. Numbers in the parentheses show the percentage contributions to the OHR_{TOTAL}.

	Location	CH_4	CO	NOx	VOCs	Total	Platform	Time Period	Reference
California	SoCAB	0.31 (5%)	1.14 (19%)	1.05 (17%)	3.59 (59%)	6.10	Aircraft	Jul, Sep 2019	This study
	SJV	0.34 (7%)	0.81 (18%)	0.32 (7%)	3.12 (68%)	4.59			
	Pasadena		2.1 (15%)	4.7 (34%)	7.1 (51%)	13.9[a]	Ground	May–Jun2010	Heald et al. (2020)
	Granite Bay	0.30 (3%)	0.77 (8%)	2.01 (22%)	6.22 (67%)	9.3	Ground	Jul–Sep 2001	Steiner et al. (2008)
	Sacramento	0.30 (3%)	0.80 (7%)	3.77 (33%)	6.61 (58%)	11.5		Summer 2000	
	Fresno	0.30 (2%)	1.86 (11%)	6.60 (38%)	8.85 (50%)	17.6		Summer 2000	
	Blodgett Forest	0.30 (3%)	0.79 (8%)	0.2 (2%)	8.09 (86%)	9.4		Jul–Sep 2001	
Gulf of Mexico/Houston	Central Gulf of Mexico	0.27 (27%)	0.39 (38%)	0.032 (3%)	0.32 (32%)	1.01	Ship	Jul–Sep 2006	Gilman et al. (2009)
	Coastal offshore	0.27 (10%)	0.61 (22%)	0.42 (15%)	1.44 (53%)	2.74			
	Houston and Galveston Bay	0.27 (3%)	0.73 (7%)	1.82 (18%)	7.25 (72%)	10.1			
Centreville, Alabama			0.86 (5%)	0.22 (1%)	15.5 (93%)	16.6[a]	Ground	Jun–Jul 2013	Heald et al. (2020)
Hong Kong	Tsuwen	0.29 (2%)	2.91 (20%)	6.08 (41%)	5.34 (37%)	14.62	Ground	Sep–Nov 2010	Ling et al. (2014)
	Mount Tai Mo Shan	0.28 (4%)	2.51 (33%)	1.77 (23%)	3.09 (40%)	7.65			
Tokyo, Japan		0.27 (1%)	2.9 (13%)	7.5 (33%)	11.4 (50%)	22.5	Ground	Jul–Aug 2003	Sadanaga et al. (2005)
Paris, France		0.35 (2%)	1.75 (11%)	9.63 (61%)	4.03 (26%)	15.8	Ground	Jan–Feb 2010	Dolgorouky et al. (2012)
North Norfolk coast, UK		0.29 (10%)	0.63 (21%)	0.72 (25%)	1.0 (35%)	2.9	Ground	Apr–May 2004	Lee et al. (2010)
Remote MBL over the Pacific and Atlantic Oceans		0.27–0.34 (19-24%)	0.42–0.56 (30-40%)			1.4[b]	Aircraft	Jul–Aug 2016 Jan–Feb 2017 Sep–Oct 2017 Apr–May 2018	Thames et al. (2020)
Remote MBL over the North Pacific Ocean		0.22 (14%)	0.93 (58%)	0.02 (1%)	0.29 (18%)	1.6[b]	Aircraft	Apr–May 2006	Mao et al. (2009)
Global mean		0.24 (31%)	0.093 (12%)	0.013 (2%)	0.43[c] (55%)	0.78	Model	Annual mean	Heald and Kroll (2020)

[a]OHR_{TOTAL} is the sum of OHR_{CO}, OHR_{NO2}, and OHR_{VOC}, not including OHR_{CH4}.

[b]OHR_{TOTAL} calculated using top-down methods.

[c]The number represents reactive organic carbon, which also includes particulate organic carbon and secondary CO.

Table S2. Comparison of the percentage contributions to the OHR_{VOC} in this study with other regions.

	Location	OVOCs	BVOCs	Alkanes	Alkenes	Aromatics	Platform	Time Period	Reference
California	SoCAB	64%	21%	7%	5%	3%	Aircraft	Jul, Sep 2019	This study
	SJV	86%	6%	3%	4%	1%			
	Pasadena	45%	20%	12%	15%	7%	Ground	May–Jun 2010	Heald et al. (2020)
Gulf of Mexico/Houston	Central Gulf of Mexico	60%	3%	9%	26%	0%	Ship	Jul–Sep 2006	Gilman et al. (2009)
	Coastal offshore	37%	3%	20%	34%	4%			
	Houston and Gaveston Bay	14%	7%	23%	41%	5%			
Houston, Texas		20%	15%	15%	28%	21%	Ground	Aug–Sep 2006	Mao et al. (2010)
La Porte, Texas		35%	6%	15%	40%	4%	Ground	Aug–Sep 2000	
New York City, New York		40%	11%	11%	26%	11%	Ground	Jun–Aug 2001	
Centreville, Alabama		14%	84%	0%	1%	0%	Ground	Jun–Jul 2013	Heald et al. (2020)
Mexico City, Mexico		17%	2%	35%	35%	11%	Ground	Apr–May 2003	Mao et al. (2010)
Hong Kong	Tsuwen	33.5%	11.3%	12.8%	24.0%	18.3%	Ground	Sep–Nov 2010	Ling et al. (2014)
	Mount Tai Mo Shan	42.8%	11.7%	9.2%	18.5%	17.6%			
Mainland China[a]		19%	1%	9%	30%	40%	Model	2013	Wu and Xie (2017)
Seoul, South Korea		19%	46%	11%	8%	16%	Ground	May–Jun 2015	Kim et al. (2018)

[a]The BVOC and OVOC data were recalculated from Table S5 in Wu and Xie (2017),(Wu and Xie, 2017) as it did not include a BVOCs category. The data represent averages of three major regions (the North China Plain, the Yangtze River Delta, and the Pearl River Delta) of China.

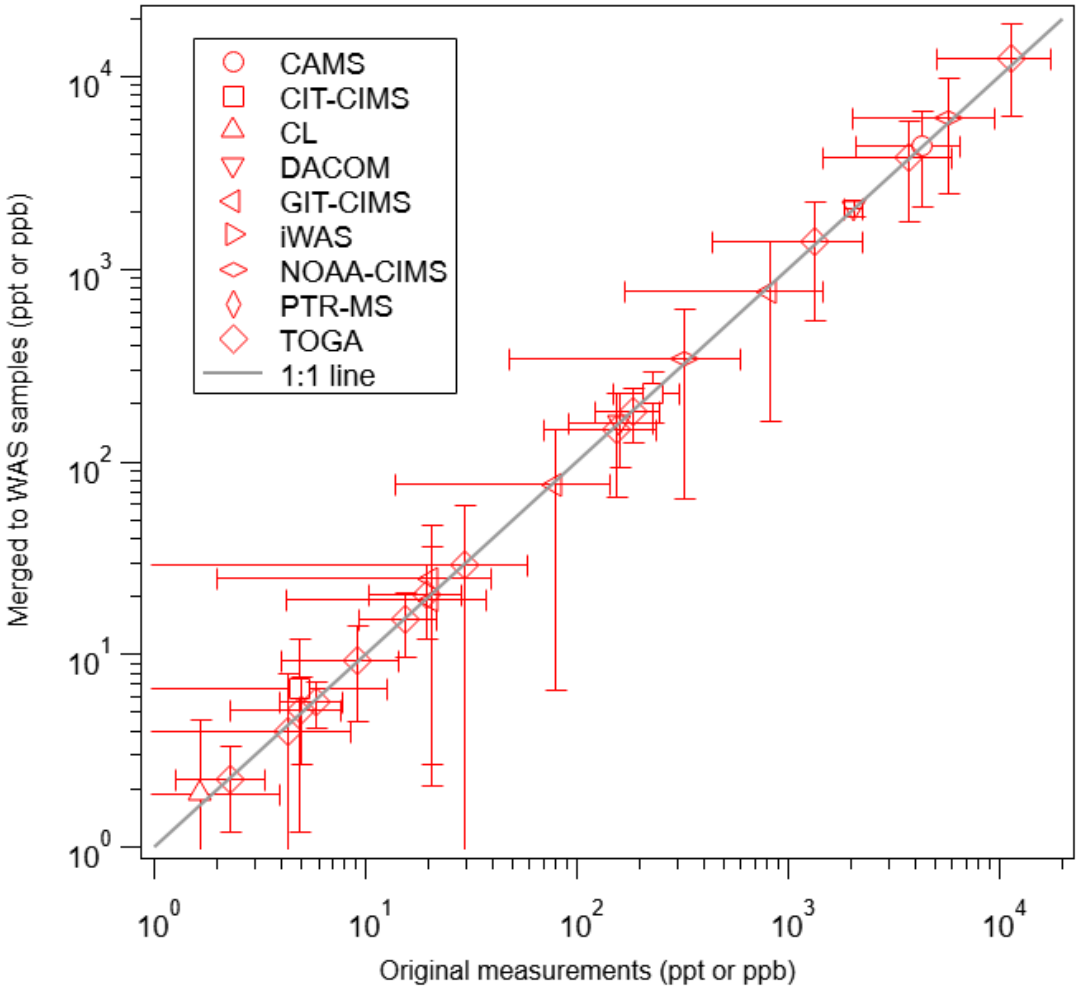

Figure S1: Comparison of the merged measurements (to the WAS intervals) with the original measurements from nine instruments (shown in the legend). The symbols represent campaign-average mixing ratios. The error bars represent the standard deviations.

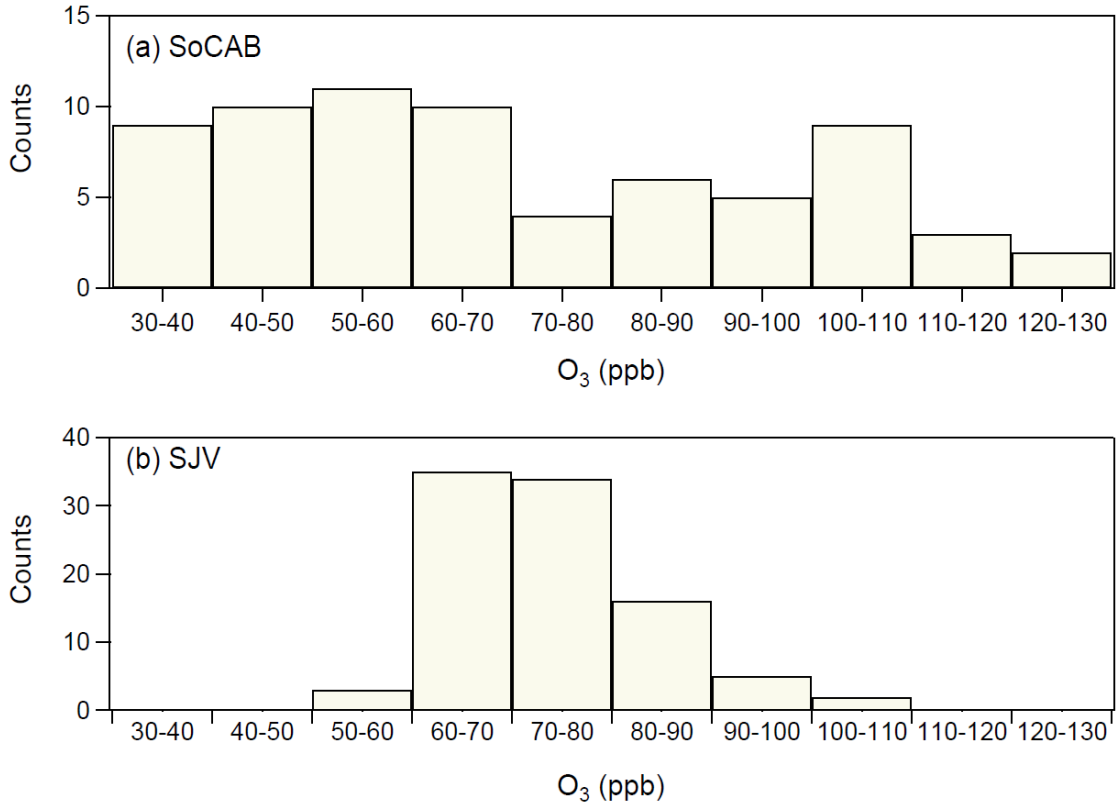

Figure S2: Frequency distribution of O_3 in the (a) SoCAB and (b) SJV.

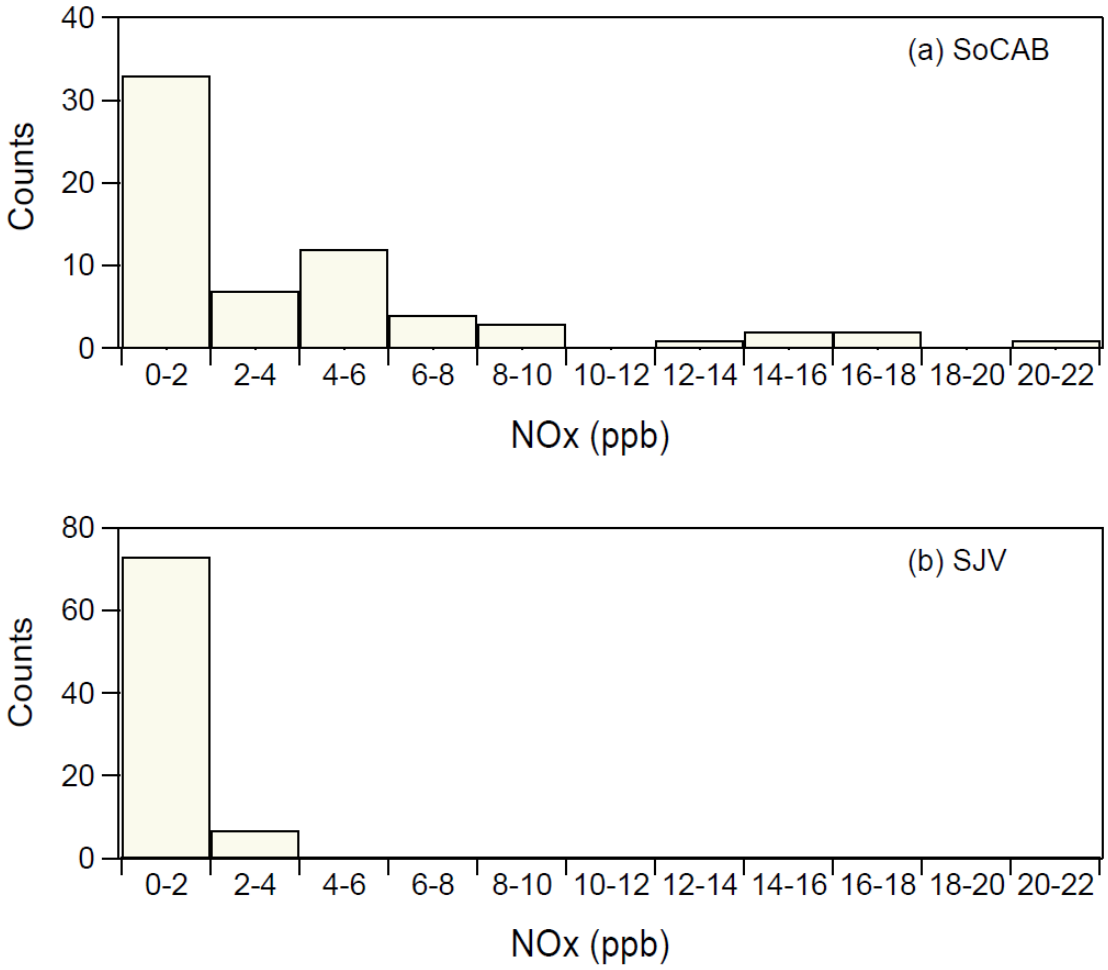

Figure S3: Frequency distribution of the NOx concentration in the (a) SoCAB and (b) SJV.

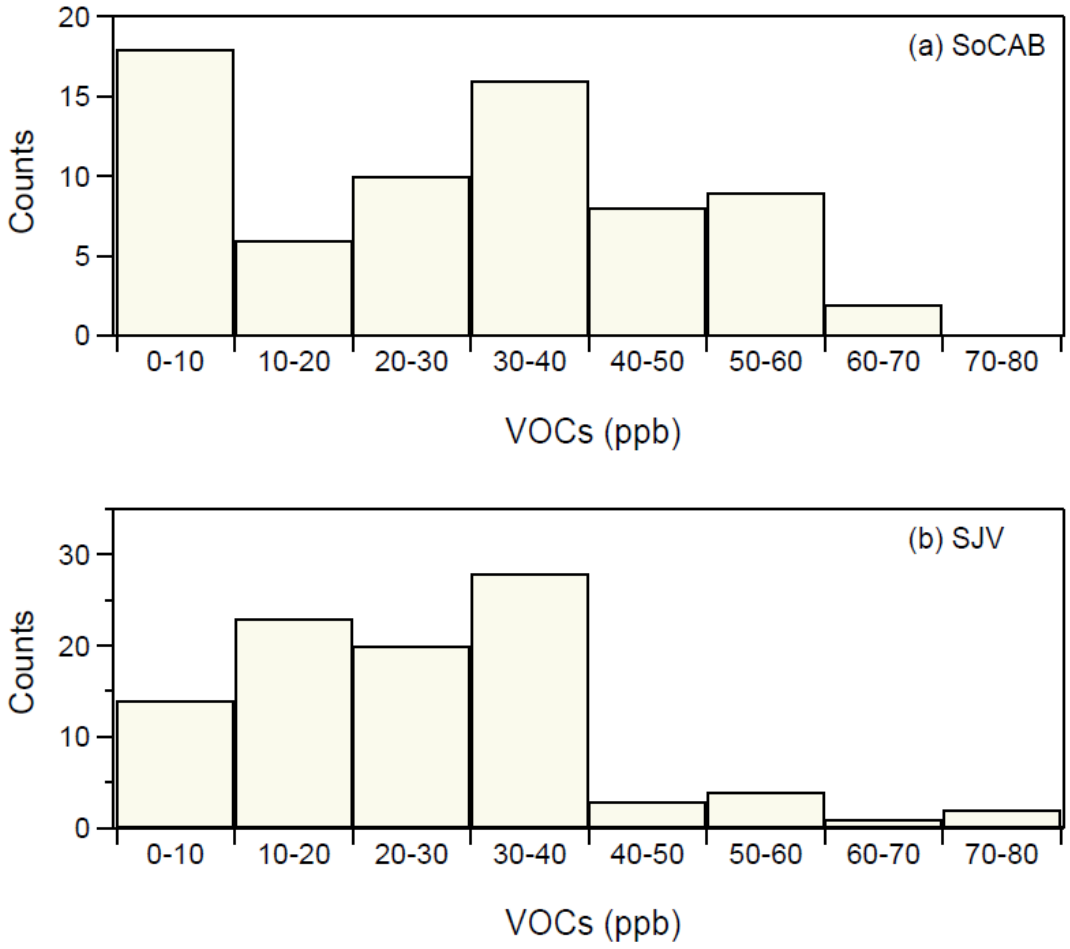

Figure S4: Frequency distribution of the total VOC concentration in the (a) SoCAB and (b) SJV.

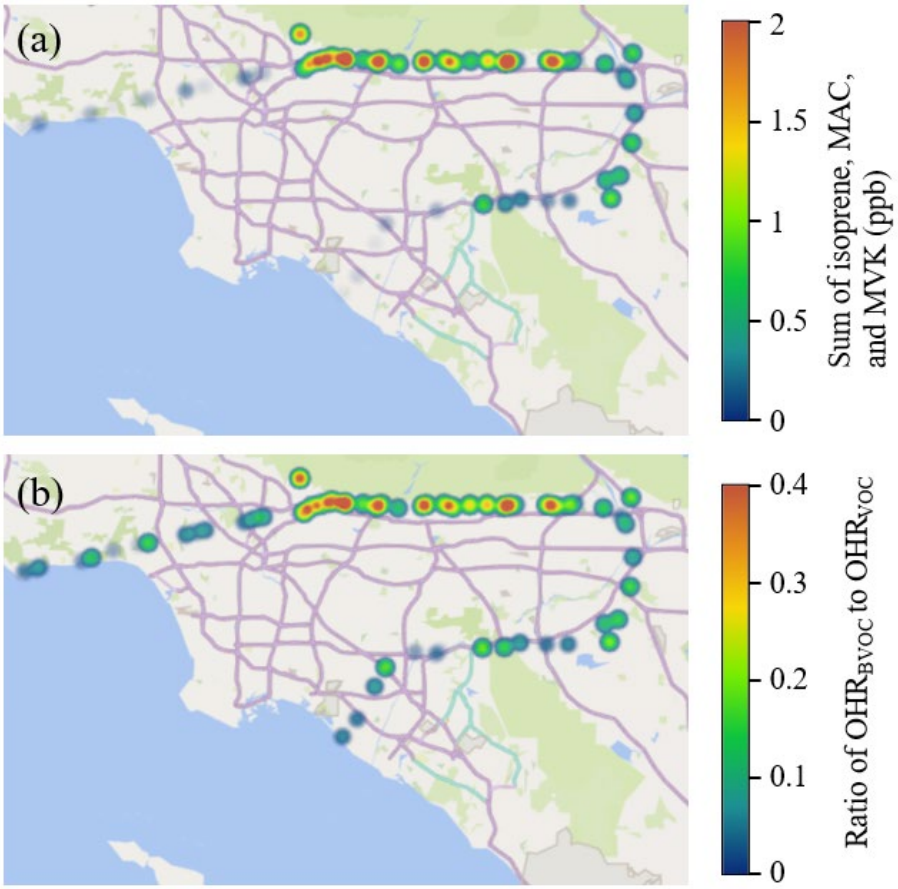

Figure S5: Spatial distribution of (a) the sum of the mixing ratio for isoprene and its oxidation products MAC and MVK, and (b) the ratio of OHR_{BVOC} to OHR_{VOC} in the SoCAB. The colors of the heatmaps are shown in the legend.